

**CHAPTER IV**  
**RESULTS AND DISCUSSION**

**4.1 Gas Separation Performance in UOP Lab**

Matrimid dense membrane and mixed matrix membranes (MMMs) containing three different inorganic fillers for gas separation were successfully fabricated at 0 wt.% (pure Matrimid), 15 wt.% and 25 wt.% using the solution-casting method. In this work, various inorganic fillers such as activated carbon,  $\gamma$ - $\text{Al}_2\text{O}_3$  and 4A zeolite were incorporated into Matrimid polymer in order to improve permeability and selectivity of the pair of gases. The obtained results of Matrimid dense membrane and MMMs are shown in Table 4.1.

**Table 4.1** Separation performances of Matrimid dense membrane and MMMs

Membrane	Gas Permeability ( Barrer)*			Gas Selectivity	
	CH <sub>4</sub>	CO <sub>2</sub>	H <sub>2</sub>	CO <sub>2</sub> /CH <sub>4</sub>	H <sub>2</sub> /CH <sub>4</sub>
Matrimid	0.36	7.9	24.7	22.0	68.6
15 wt.% AC/ Matrimid	0.55	13.7	39.9	25.0	72.8
25 wt.% AC/ Matrimid	1.41	24.2	67.3	17.2	47.7
15 wt.% $\gamma$ -Al <sub>2</sub> O <sub>3</sub> / Matrimid	0.86	15.4	46.1	18.0	53.9
25 wt.% $\gamma$ -Al <sub>2</sub> O <sub>3</sub> / Matrimid	1.67	25.4	80.9	15.2	48.4
15 wt.% 4A/ Matrimid	0.70	12.2	39.9	17.5	57.2
25 wt.% 4A/ Matrimid	3.04	15.8	52.1	5.2	17.1

\*Permeability (Barrer) =  $1 \times 10^{-10} \text{ cm}^3 \text{ (STP) cm/ cm}^2 \cdot \text{sec} \cdot \text{cmHg}$

Permeancen (GPU) =  $1 \times 10^{-6} \text{ cm}^3 \text{ (STP)/cm}^2 \cdot \text{sec} \cdot \text{cmHg}$

The relationship between gas permeance and gas permeability is shown in Appendix A. The gas permeance of the tested gases and the selectivity of the gas pairs (CO<sub>2</sub>/CH<sub>4</sub> and H<sub>2</sub>/CH<sub>4</sub>) for Matrimid dense membrane and MMMs are also provided in Appendix B.

#### 4.1.1 Gas Permeability and CO<sub>2</sub>/CH<sub>4</sub> Selectivity in Matrimid Dense Membrane and MMMs

##### 4.1.1.1 *Pure Matrimid Dense Membrane*

The diffusivity term is usually dominant for separation properties in glassy polymer refer to the permeability falls with increasing molecular size and smaller molecule permeates preferentially (Othmer *et al.*, 1981). For pure Matrimid dense membrane, the gas permeabilities of H<sub>2</sub>, CO<sub>2</sub> and CH<sub>4</sub> are 24.7, 7.94 and 0.36 Barrer, respectively. The gas molecules with smaller diameter have higher permeability in the order of the permeability of H<sub>2</sub> > CO<sub>2</sub> > CH<sub>4</sub> corresponding kinetic diameters of 2.89, 3.3, and 3.8 Å, respectively. According to the solution-diffusion mechanism, an increase in permeability is controlled by the polymer chain mobility that allows the preferential diffusion of certain gas molecules based on their sizes and shapes of the gases. The solubility of gas in polymer depends on the condensability of the penetrant and the extent of the polymer-penetrant interaction. The condensability of the gases increases in the order of H<sub>2</sub> < CH<sub>4</sub> < CO<sub>2</sub> according to their critical temperatures (Ordonez, *et al.*, 2010). The critical temperatures of H<sub>2</sub>, CH<sub>4</sub> and CO<sub>2</sub> are -240.2, -82.1 and 31 °C, respectively (Shekhawat *et al.*, 2003). Due to the condensable nature of CO<sub>2</sub> and its good interaction with the polar segments of Matrimid polymer, Matrimid is more selective to CO<sub>2</sub> than CH<sub>4</sub> and the values of CO<sub>2</sub>/CH<sub>4</sub> selectivity is 22.

##### 4.1.1.2 *4A Zeolite-Matrimid MMMs*

It can be seen from Figure 4.1 that the incorporation of zeolite into Matrimid polymer resulted in increasing permeabilities of H<sub>2</sub>, CO<sub>2</sub> and CH<sub>4</sub> as the loading of inorganic fillers was increased. This is because molecular sieving characteristic played a dominant role in transport mechanism beside the solution-diffusion mechanism which is a fundamental one in polymeric membrane.

However, the selectivity of  $\text{CO}_2/\text{CH}_4$  was decreased with increasing inorganic loading. This increase of permeability combined with a decrease in selectivity may be due to the formation of non-selective interfacial voids at the interface of polymer and inorganic fillers because of poor adhesion (Aroon *et al.*, 2010). Moreover, the selectivity of  $\text{CO}_2$  gas significantly decreased at 25 wt.% 4A/Matrimid as a result of more void formation occurred at a higher zeolite loading. Therefore, more methane would bypass through the formed voids at the interface of 4A zeolite and Matrimid, and the permeability of methane noticeably increased at 25 wt.% 4A/Matrimid. As these results, the selectivity of  $\text{CO}_2$  gas considerably decreased at 25 wt.% 4A/Matrimid comparing with pure Matrimid and 15 wt.% zeolite loading. These results were in good agreement with those acquired by Ahmad and Hagg (2013).

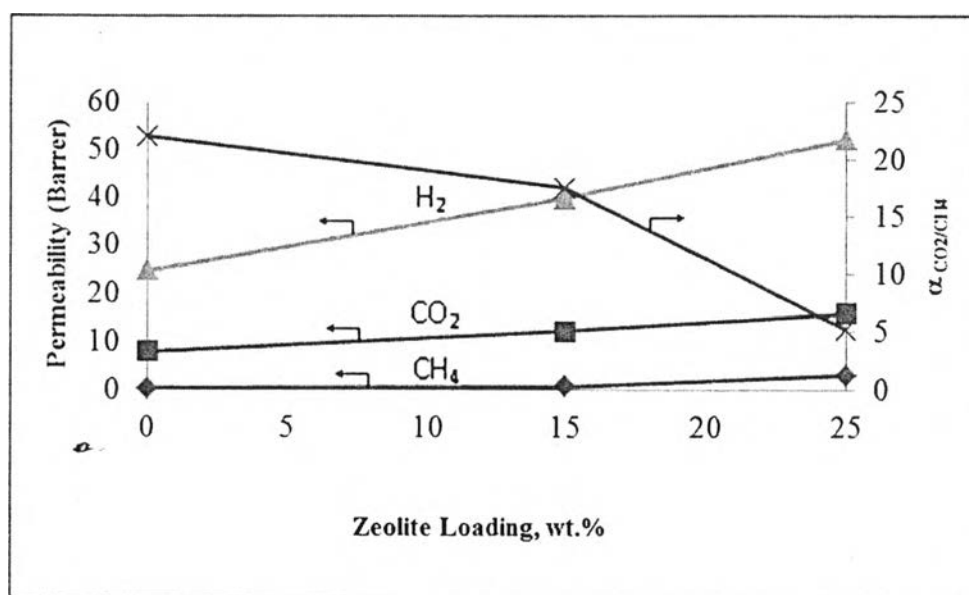


**Figure 4.1** Gas permeability and  $\text{CO}_2/\text{CH}_4$  selectivity of 4A zeolite-Matrimid MMMs.

Many researchers have identified challenges to obtain good zeolite-polymer compatibility with glassy polymer, especially polyimide. For high glass transition temperature ( $T_g$ ) polymers, the rigid polymer backbone always creates some difficulties that result in poor adhesion between polymer and zeolite particles (Vankelecom *et al.*, 1995). MMMs fabricating from such glassy polymer

showed poor zeolite-polymer contact, resulting non-selective voids and no selectivity improvement. Moreover, stresses generated during removal of solvent, tend to be large for a rigid material like Matrimid (Mahajan *et al.*, 2002). If the stress directions are not uniform around the inorganic particles, interface voids will be formed in the particle-polymer interface (Aroon *et al.*, 2010).

#### 4.1.1.3 $\gamma$ -Al<sub>2</sub>O<sub>3</sub>-Matrimid MMMs

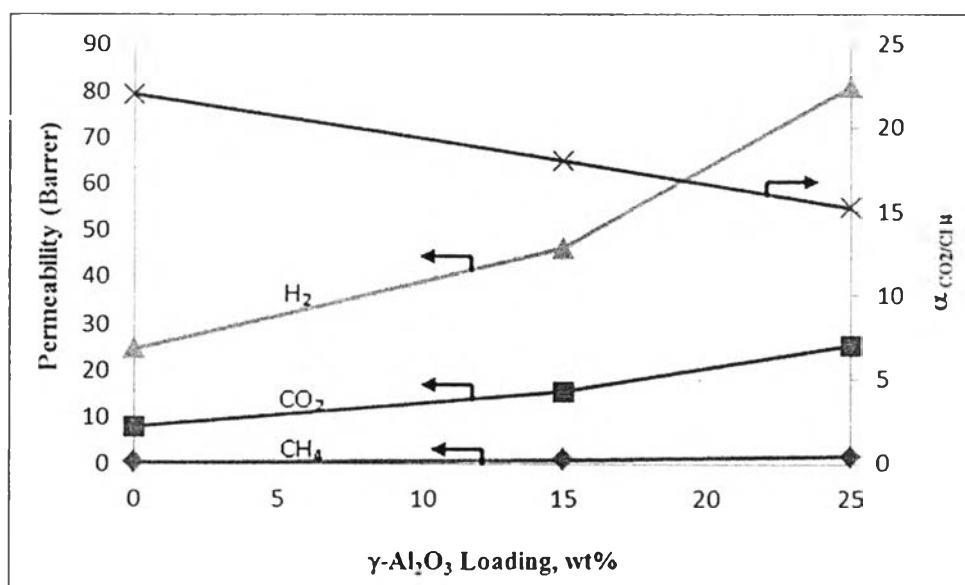


**Figure 4.2** Gas permeability and CO<sub>2</sub>/CH<sub>4</sub> selectivity of  $\gamma$ -Al<sub>2</sub>O<sub>3</sub>-Matrimid MMMs.

From Figure 4.2, the incorporation of  $\gamma$ -Al<sub>2</sub>O<sub>3</sub> into Matrimid polymer also shows the same trend as in the case of zeolite-Matrimid MMMs, increasing permeability associated with decreasing selectivity. The results obtained could be explained the same reasons as the non-selective interfacial voids. Generally, the mesoporous structure of alumina dictates that transport within membranes fabricated from it will take place by a Knudsen diffusion mechanism (Shekhawat *et al.*, 2003). However the CO<sub>2</sub>/CH<sub>4</sub> selectivity falls slightly with increasing  $\gamma$ -Al<sub>2</sub>O<sub>3</sub> loading into Matrimid clarifies that poor interfacial adhesion between  $\gamma$ -Al<sub>2</sub>O<sub>3</sub> and Matrimid polymer is not severe.

#### 4.1.1.4 Activated Carbon-Matrimid MMMs

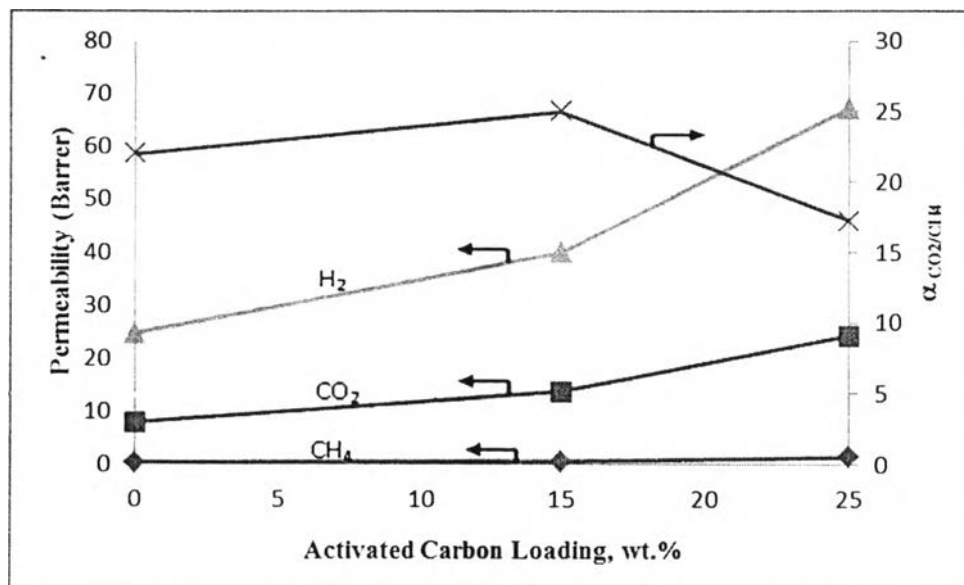


**Figure 4.3** Gas permeability and CO<sub>2</sub>/CH<sub>4</sub> selectivity of activated carbon-Matrimid MMMs.

As shown in Figure 4.3, the incorporation of activated carbon into Matrimid polymer results in increasing permeabilities of H<sub>2</sub>, CO<sub>2</sub> and CH<sub>4</sub> as the loading of activated carbons was increased. Interestingly, both permeability and selectivity of CO<sub>2</sub> are increased at 15 wt.% activated carbons loaded in Matrimid polymer comparing with Matrimid membrane. Permeation measurements showed CO<sub>2</sub> permeability and CO<sub>2</sub>/CH<sub>4</sub> selectivity of activated carbon-Matrimid MMMs with 15 wt.% loading of activated carbon up to 13.7 Barrer and 25 respectively. Correspondingly, the CO<sub>2</sub> permeability and CO<sub>2</sub>/CH<sub>4</sub> selectivity increase with 73 % and 14 % over the pure polymer. This might be because the adsorbability of penetrant is a key separation character of activated carbons. These results could be partially considered the mechanism of preferential surface diffusion of CO<sub>2</sub> (more adsorbable gas) over the CH<sub>4</sub> gas (less adsorbable compound). Furthermore, typical activated carbons have higher adsorption selectivity for CO<sub>2</sub> (polar gas) than for CH<sub>4</sub> (non-polar compound) (Anson *et al.*, 2004).

#### 4.1.2 Comparison of Separation Performance among 4A Zeolite-Matrimid, $\gamma$ -Al<sub>2</sub>O<sub>3</sub>-Matrimid and Activated Carbon-Matrimid MMMs

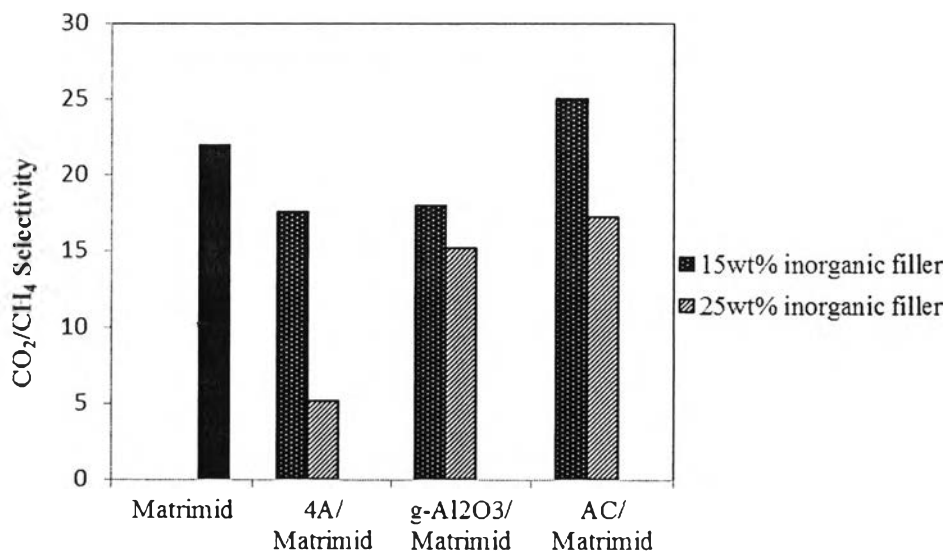


**Figure 4.4** CO<sub>2</sub>/CH<sub>4</sub> selectivity among 4A zeolite-Matrimid,  $\gamma$ -Al<sub>2</sub>O<sub>3</sub>-Matrimid and activated carbon-Matrimid MMMs.

The comparison of CO<sub>2</sub>/CH<sub>4</sub> selectivity among 4A zeolite-Matrimid,  $\gamma$ -Al<sub>2</sub>O<sub>3</sub>-Matrimid and activated carbon-Matrimid MMMs is presented in Figure 4.4. It can be clearly seen that CO<sub>2</sub>/CH<sub>4</sub> selectivity over MMMs decreases with increasing inorganic loading excepting 15 wt.% activated carbon-Matrimid MMMs as compared to the pure Matrimid membrane. This may be the stronger interaction between activated carbon and Matrimid and higher adsorption selectivity of activated carbon for CO<sub>2</sub> than CH<sub>4</sub>. These results led to the enhancement of the gas separation performance of activated carbon-Matrimid MMMs.

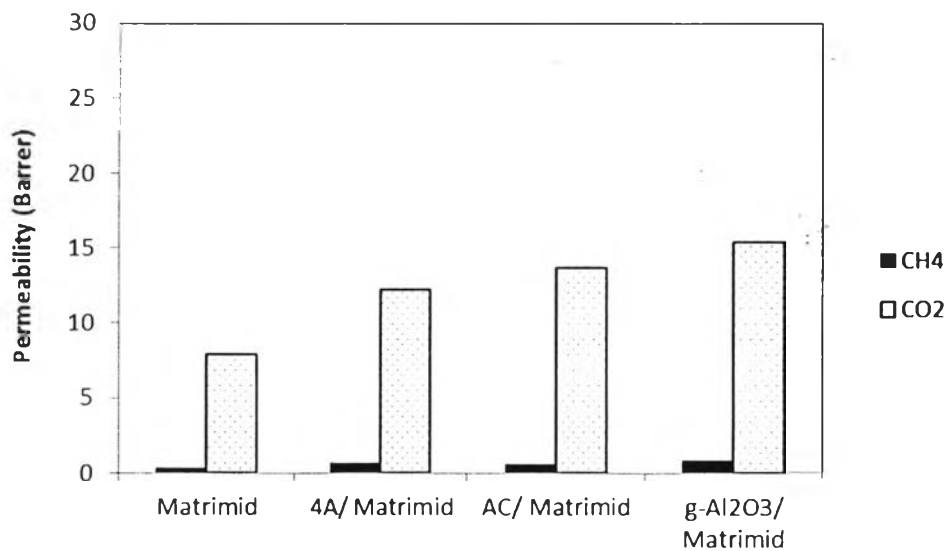


**Figure 4.5** The gas permeabilities of pure Matrimid membrane and 15 wt.% inorganic filler-Matrimid MMMs.

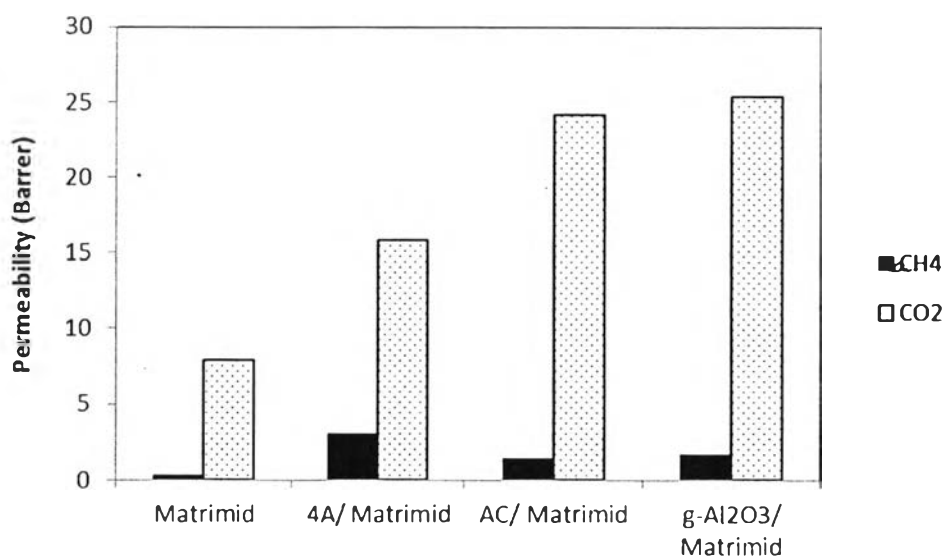


**Figure 4.6** The gas permeabilities of pure Matrimid membrane and 25 wt.% inorganic filler-Matrimid MMMs.

By comparing 4A zeolite-Matrimid and  $\gamma$ -Al<sub>2</sub>O<sub>3</sub>-Matrimid MMMs, the declination of CO<sub>2</sub>/CH<sub>4</sub> selectivity is approximately similar at the 15 wt.% inorganic loading. However zeolite-Matrimid gas separation suffers from defects caused by poor contact between inorganic-Matrimid interface more severe than  $\gamma$ -Al<sub>2</sub>O<sub>3</sub>-Matrimid at 25 wt.% inorganic loading. This may be due to the precipitation of zeolites that may occur during the MMM fabrication. High zeolite loading could lead to more sedimentation of zeolite particles and bigger chance of voids formation during membrane fabrication (Bastani *et al.*, 2013). Consequently, methane, the bigger molecule, would pass through the formed voids at the interface of 4A zeolite and Matrimid, and a dramatic decrease in CO<sub>2</sub>/CH<sub>4</sub> selectivity (Figure 4.4) combined with an intense increase in CH<sub>4</sub> permeability (Figure 4.6) ensues at 25 wt.% 4A/Matrimid. On the other hand, CO<sub>2</sub>/CH<sub>4</sub> selectivity decreases slightly corresponding with increasing gamma-alumina loading and thus  $\gamma$ -Al<sub>2</sub>O<sub>3</sub>-Matrimid MMMs shows better interfacial contact than 4A-Matrimid MMMs.

The effect of inorganic filler loading on the permeabilities of the tested gases for inorganic filler-Matrimid MMMs comparing with pure Matrimid membrane are presented in Figures 4.5 and 4.6 respectively. The permeabilities of the tested gases show a consistently parallel behaviour in which the permeabilities of CO<sub>2</sub> and CH<sub>4</sub> increase with increasing inorganic loading. However a different tendency that the permeability of CH<sub>4</sub> significantly rises in 25 wt.% 4A zeolite-Matrimid MMMs is observed. The cause of this peculiar behaviour was clarified with CO<sub>2</sub>/CH<sub>4</sub> selectivity illustrated in Figure 4.4 above.

#### **4.2. Differences in Fabrication Aspects at UOP and PPC**

The results obtained in UOP lab showed that the permeability of MMMs increased for CO<sub>2</sub> gas with corresponding decrease in their selectivity over CH<sub>4</sub> as the loading of inorganic fillers was increased. This increase of permeability combined with a decrease in selectivity may be due to the formation of non-selective interfacial voids at the interface of polymer and inorganic fillers because of poor adhesion (Aroon *et al.*, 2010).



Two factors seem to be critical to the formation of the interface: the nature of the polymer-sieve interaction, and the stress encountered during material preparation. The latter, stresses, generated during removal of solvent will tend to be large for a rigid material like Matrimid (Mahajan *et al.*, 2002). In this work, only the stress encountered during membrane fabrication was focused on and gamma-alumina was selected as the inorganic filler. Alumina finds its use in the separation of gases mainly as a support, where its sound structural properties, and chemical and hydrothermal stabilities beyond 1,000 °C make it very desirable (Shekhawat *et al.*, 2003). Gamma-alumina as an inorganic filler in MMMs is rarely seen in the literature. However  $\gamma$ -Al<sub>2</sub>O<sub>3</sub>-Matrimid MMMs indicated better interfacial contact than 4A-Matrimid MMMs in our previous work at UOP. The properties of gamma-alumina are shown in Table 4.2.

**Table 4.2** The properties of gamma-alumina (UOP Versal™ Alumina, UOP)

Loose Bulk Density (kg/m <sup>3</sup> )	Surface Area (m <sup>2</sup> /g)	Pore Volume (cm <sup>3</sup> /g)
193	150-250	1.32-1.36

To emphasize the second factor mentioned above, the different fabrication procedures in UOP lab and PPC lab are listed as follows: solvent selection, priming, casting, evaporation and drying steps.

Two solvents i.e., NMP and 1, 3-dioxolane were used in UOP lab and only one solvent (1, 3-dioxolane) was used in PPC lab where it was difficult to get defect-free pure Matrimid membrane and MMMs using the mixture of the solvents. Polymer shrinkage could be occurred when the solution was cast and dried in fabricating pure Matrimid membrane. It may be because of different boiling point solvents and the evaporation rates are not the same. Although the nascent membranes were heated on a hot plate and dried in a vacuum oven in UOP lab, an atmospheric vacuum oven was used in PPC lab for drying the membranes. That the membrane

solution had been cast and put in an atmospheric oven at once may cause the fast evaporation of low boiling point solvent. However only low boiling point solvent such as 1, 3-dioxolane is easy to control polymer shrinkage in PPC lab. Moreover, low boiling point solvent has the advantage of requiring less evaporation time and energy consumption as well as the sedimentation of the inorganic filler can be expected to decrease (Ahmad and Hagg, 2013).

In spite of adding a half of the polymer to the solution of gamma-alumina and solvent as prepared MMMs in UOP lab, 15 wt.% of the total polymer was added to the solution fabricated in PPC lab in order to be primed. Coating the surface of the inorganic particles with a dilute polymer dope prior to the dispersion in the bulk polymer, is known as a priming method. This method can reduce any stress at the polymer-particle interface. In the priming technique, particles are mixed in a suitable solvent and a small percentage of the total polymer, used to form a membrane polymer solution (typically 5–15 wt.%), is added to a suspension of particles. Prior to the addition of the bulk polymer solution, thorough mixing between the priming polymer and the suspension of the polymer particles effectively coats the dispersed phase particles. This technique minimizes agglomeration of the particles and promotes interaction between the bulk polymer and polymer primed particles, thereby minimizing defective interfaces (Aroon *et al.*, 2010).

Despite being cast the membrane solution on a clean glass plate at 55 °C on a hot plate and heated overnight in UOP lab, the solution was cast at room temperature and dried in the box saturated with the solvent for 24 h to delay solvent evaporation. After that the nascent membrane was heated in an oven at 80 °C for 12 h in order to remove the remaining solvent in the membrane.

The thickness of membranes was adjusted by a casting knife at 20 mil in UOP lab and 10 mil in PPC lab in order to increase the rate of permeation. For high rates of production, the dense separating layer of the membrane must be as thin as possible, yet strong enough to withstand considerable transmembrane pressure differential driving forces (Husain and Koros, 2007).

Overall, the variation of environmental conditions, for example, humidity, temperature and pressure within or between the laboratories and different

apparatuses may influence the fabrication steps of membranes to have defect-free membranes in PPC lab as compared to the preparing procedures used in UOP lab.

### 4.3 Membrane Characterization at PPC

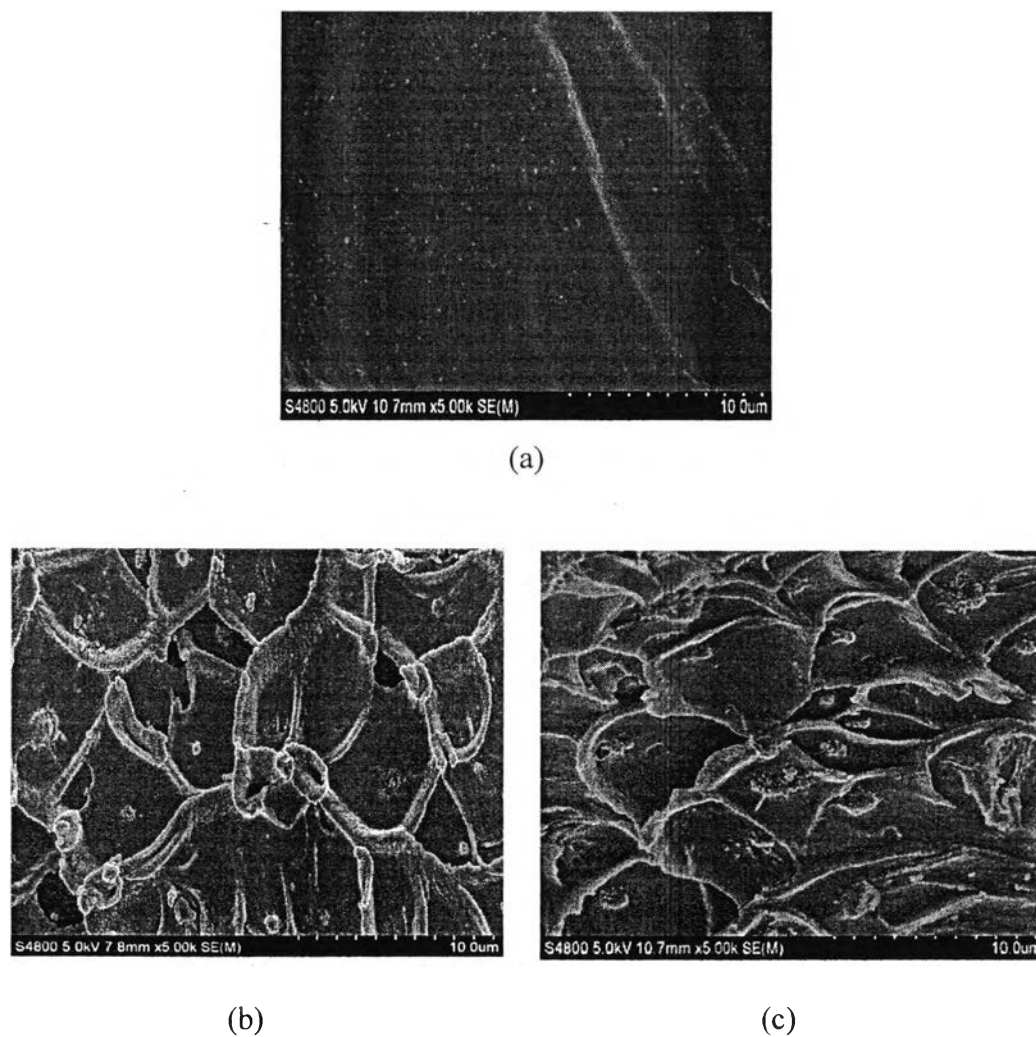


**Figure 4.7** SEM images of cross sectional (a) pure Matrimid membrane (b) 15 wt.%  $\gamma$ -Al<sub>2</sub>O<sub>3</sub>-Matrimid and (c) 25 wt.%  $\gamma$ -Al<sub>2</sub>O<sub>3</sub>-Matrimid.

Scanning electron microscopy (SEM) was performed using a FESEM (Hitachi S4800). Cross sections of pure Matrimid membrane and  $\gamma$ -Al<sub>2</sub>O<sub>3</sub>-Matrimid MMMs were prepared by the freeze-fracture of the membranes after immersing a

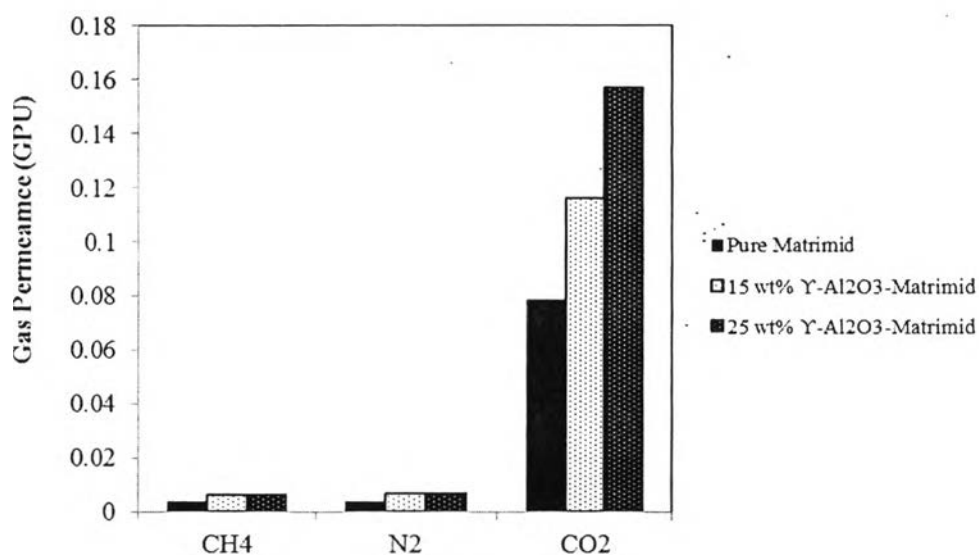
few minutes in liquid nitrogen and subsequent sputter-coating with a thin layer of platinum.

Figure 4.7 (a) shows that the SEM image of cross sectional pure Matrimid membrane indicates a good homogeneity of polymer. From Figures 4.7, (b) and (c), those of 10 wt.% and 25 wt.% of  $\gamma$ -Al<sub>2</sub>O<sub>3</sub> present a small agglomeration of inorganic particles in Matrimid polymer. Particularly, the crater-like structure which indicates adequate compatibility between the polymer and particles can be observed in the  $\gamma$ -Al<sub>2</sub>O<sub>3</sub>-Matrimid MMMs. Indeed, strong interaction of particles with polymer chains makes interfacial stress during membranes fracturing in liquid nitrogen as a procedure in SEM analysis. This stress deforms polymer matrices and makes a crater-like structure in which particles are at the center of it (Dorosti *et al.*, 2014 and Zhang *et al.*, 2008).

#### 4.4 Gas Separation Performance in PPC Lab

MMMs incorporating  $\gamma$ -Al<sub>2</sub>O<sub>3</sub> into Matrimid polymer were attemptedly fabricated at 0 wt.% (pure Matrimid), 15 wt.% and 25 wt.%  $\gamma$ -Al<sub>2</sub>O<sub>3</sub> loading via the solution-casting method. The separation performance of MMMs was examined by single gas permeation measurements using a bubble flow meter according to the sequential testing of nitrogen (N<sub>2</sub>), methane (CH<sub>4</sub>) and carbon dioxide (CO<sub>2</sub>). Single gas permeance and ideal gas selectivity determined from a flow rate of each gas at steady state through the  $\gamma$ -Al<sub>2</sub>O<sub>3</sub>-Matrimid MMMs at room temperature and 100 psi are shown in Figures 4.8 and 4.9, respectively.

As presented in Figure 4.8, the permeance of nitrogen (N<sub>2</sub>), methane (CH<sub>4</sub>) and carbon dioxide (CO<sub>2</sub>) increases with increasing gamma-alumina loading in the order of CH<sub>4</sub> < N<sub>2</sub> < CO<sub>2</sub>. The corresponding kinetic diameters of the tested CH<sub>4</sub>, N<sub>2</sub> and CO<sub>2</sub> gases are 3.8, 3.64 and 3.3 Å, respectively. The permeances of CO<sub>2</sub> for 0 wt.%, 15 wt.% and 25wt.%  $\gamma$ -Al<sub>2</sub>O<sub>3</sub>-Matrimid MMMs are 0.0787, 0.1159 and 0.1570 GPU, respectively, while those of N<sub>2</sub> are 0.0039, 0.0068 and 0.0070 GPU and those of CH<sub>4</sub> are 0.0035, 0.0062 and 0.0065 GPU, respectively as provided in Appendix C.



**Figure 4.8** Gas permeance of the tested gases for pure Matrimid and  $\gamma$ -Al<sub>2</sub>O<sub>3</sub>-Matrimid MMMs at room temperature and 100 psi.

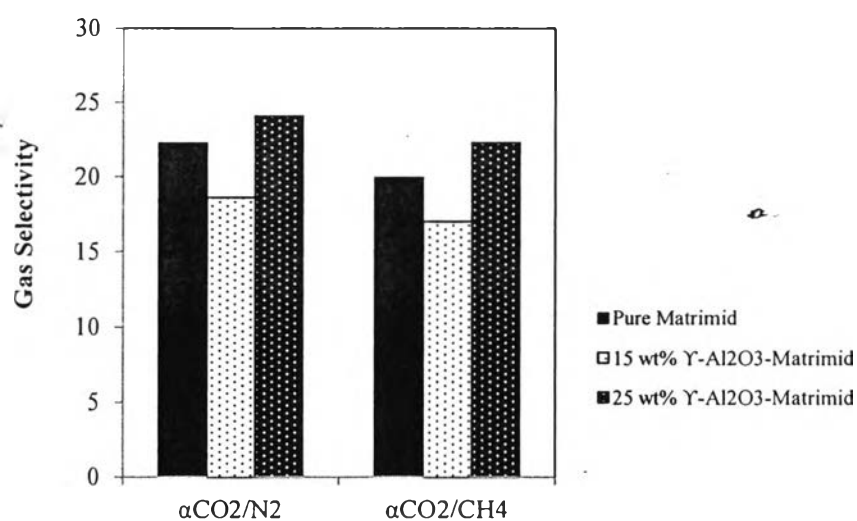


**Figure 4.9** Gas selectivity of pure Matrimid and  $\gamma$ -Al<sub>2</sub>O<sub>3</sub>-Matrimid MMMs at room temperature and 100 psi.

It can be clearly observed from Figure 4.9 that  $\text{CO}_2/\text{CH}_4$  and  $\text{CO}_2/\text{N}_2$  selectivities of 15 wt.%  $\gamma\text{-Al}_2\text{O}_3$ -Matrimid MMM are decreased as compared to pure Matrimid. However, incorporation of  $\gamma\text{-Al}_2\text{O}_3$  into Matrimid polymer resulted in increasing permeabilities of  $\text{N}_2$ ,  $\text{CO}_2$  and  $\text{CH}_4$ . Therefore, the 15 wt.%  $\gamma\text{-Al}_2\text{O}_3$ -Matrimid MMM may be suffered from some defects, non-selective interfacial voids at the interface of polymer and particles because of some deficiency, poor adhesion, in membrane fabrication.

On the other hand,  $\text{CO}_2/\text{CH}_4$  and  $\text{CO}_2/\text{N}_2$  selectivities of the 25 wt.%  $\gamma\text{-Al}_2\text{O}_3$ -Matrimid MMM are significantly increased with increasing  $\gamma\text{-Al}_2\text{O}_3$  loading. Although a small cluster of particles could occur in both  $\gamma\text{-Al}_2\text{O}_3$ -Matrimid MMMs according to SEM images, interfacial void formation in the 25 wt.%  $\gamma\text{-Al}_2\text{O}_3$ -Matrimid MMM might be less than the 15 wt.%  $\gamma\text{-Al}_2\text{O}_3$ -Matrimid MMM. Consequently, the 25 wt.%  $\gamma\text{-Al}_2\text{O}_3$ -Matrimid MMM enhances the gas separation performance as compared to the 15 wt.%  $\gamma\text{-Al}_2\text{O}_3$ -Matrimid MMM even though its selectivity slightly increases in comparison with the pure Matrimid polymer. The values of  $\text{CO}_2/\text{CH}_4$  selectivity for pure Matrimid, 15 wt.% and 25wt.%  $\gamma\text{-Al}_2\text{O}_3$ -Matrimid MMMs are 22.2, 18.6, and 24.1 while those of  $\text{CO}_2/\text{N}_2$  selectivity are 19.9, 17.0, and 22.3 respectively as provided in Appendix D.

The 25 wt.%  $\gamma\text{-Al}_2\text{O}_3$ -Matrimid MMM might be an adequate compatibility at the filler/Matrimid polymer interface as the permeance of the tested gases and the selectivity of the gas pairs ( $\text{CO}_2/\text{CH}_4$  and  $\text{CO}_2/\text{N}_2$ ) increased simultaneously. Therefore, these results, increasing permeance combined with increasing gas selectivity at a higher  $\gamma\text{-Al}_2\text{O}_3$  loading, might not be because of a Knudsen diffusion mechanism which generally takes place in the mesoporous structure of alumina. Knudsen diffusion occurs in the gas phase through the pores in the membrane layer having diameters ( $d$ ) smaller than the mean free path dimensions of the molecules ( $\lambda$ ) in the gas mixture i.e., the Knudsen number ( $\lambda/d$ ) is much greater than one. As a result, the movement of molecules inside the narrow pore channels takes place through collision of the diffusing molecules with the surface (wall) rather than with each other. The relative permeation rate of each component is inversely proportional to the square root of its molecular weight. The molecular weights of  $\text{CO}_2$ ,  $\text{N}_2$ ,  $\text{CH}_4$

and H<sub>2</sub> are 44.01, 28.01, 16.04 and 2.02, respectively. According to Knudsen diffusion, N<sub>2</sub> molecules preferentially permeate in the case of CO<sub>2</sub>/N<sub>2</sub> separation. The selectivities of CO<sub>2</sub> with respect to N<sub>2</sub>, CH<sub>4</sub>, and H<sub>2</sub> by Knudsen diffusion will be 0.8, 0.6, and 4.7, respectively. Hence, the selectivity of CO<sub>2</sub> achieved by the Knudsen diffusion mechanism is very low and not attractive in this particular gas mixture (Shekhawat *et al.*, 2003). Nevertheless,  $\gamma$ -Al<sub>2</sub>O<sub>3</sub>-Matrimid MMMs in this study increased both permeance of CO<sub>2</sub> and the selectivity of gas pairs (CO<sub>2</sub>/CH<sub>4</sub> and CO<sub>2</sub>/N<sub>2</sub>) with increasing gamma-alumina loading. The values of CO<sub>2</sub>/N<sub>2</sub> selectivity for 15 wt.% and 25wt.%  $\gamma$ -Al<sub>2</sub>O<sub>3</sub>-Matrimid MMMs are 17.0 and 22.3, respectively and those of CO<sub>2</sub>/CH<sub>4</sub> selectivity are 18.6 and 24.1, respectively which are significantly higher than Knudsen ideal separation factor (0.8 and 0.6). This might be because of molecular sieving mechanism, surface diffusion mechanism or a combination of such mechanisms. If the inorganic filler is porous, it has the effect of molecular sieve, separating gases by their size or shape. The resulting membrane is characterized by higher permeability and selectivity of desired components. In case of pore size significantly larger than the size of molecule, adsorption and selective surface flow mechanism is to be considered as well (Bastani *et al.*, 2013). However more reasonable causes such as possible separation mechanisms and interaction between gamma-alumina and Matrimid polymer should be investigated to clarify the improvement of MMM performance.